

2018

The spatial sensitivity of the spectral diversity–biodiversity relationship: an experimental test in a prairie grassland

Ran Wang

University of Alberta, rw6@ualberta.ca

John A. Gamon

University of Nebraska-Lincoln, jgamon@gmail.com

Jeannine Cavender-Bares

University of Minnesota

Philip A. Townsend

University of Wisconsin-Madison

Arthur I. Zygielbaum

University of Nebraska-Lincoln, aiz@unl.edu


Follow this and additional works at: <https://digitalcommons.unl.edu/natrespapers>

Part of the [Natural Resources and Conservation Commons](#), [Natural Resources Management and Policy Commons](#), and the [Other Environmental Sciences Commons](#)

Wang, Ran; Gamon, John A.; Cavender-Bares, Jeannine; Townsend, Philip A.; and Zygielbaum, Arthur I., "The spatial sensitivity of the spectral diversity–biodiversity relationship: an experimental test in a prairie grassland" (2018). *Papers in Natural Resources*. 827.
<https://digitalcommons.unl.edu/natrespapers/827>

This Article is brought to you for free and open access by the Natural Resources, School of at DigitalCommons@University of Nebraska - Lincoln. It has been accepted for inclusion in Papers in Natural Resources by an authorized administrator of DigitalCommons@University of Nebraska - Lincoln.

The spatial sensitivity of the spectral diversity–biodiversity relationship: an experimental test in a prairie grassland

RAN WANG ^{1,6} JOHN A. GAMON,^{1,2,3} JEANNINE CAVENDER-BARES,⁴
PHILIP A. TOWNSEND,⁵ AND ARTHUR I. ZYGIELBAUM³

¹Department of Earth and Atmospheric Sciences, University of Alberta, Edmonton, Alberta T6G 2E3 Canada

²Department of Biological Sciences, University of Alberta, Edmonton, Alberta T6G 2E9 Canada

³School of Natural Resources, University of Nebraska, Lincoln, Nebraska 68583 USA

⁴Department of Ecology, Evolution and Behavior, University of Minnesota, Saint Paul, Minnesota 55108 USA

⁵Department of Forest and Wildlife Ecology, University of Wisconsin-Madison, Madison, Wisconsin 53706 USA

Abstract. Remote sensing has been used to detect plant biodiversity in a range of ecosystems based on the varying spectral properties of different species or functional groups. However, the most appropriate spatial resolution necessary to detect diversity remains unclear. At coarse resolution, differences among spectral patterns may be too weak to detect. In contrast, at fine resolution, redundant information may be introduced. To explore the effect of spatial resolution, we studied the scale dependence of spectral diversity in a prairie ecosystem experiment at Cedar Creek Ecosystem Science Reserve, Minnesota, USA. Our study involved a scaling exercise comparing synthetic pixels resampled from high-resolution images within manipulated diversity treatments. Hyperspectral data were collected using several instruments on both ground and airborne platforms. We used the coefficient of variation (CV) of spectral reflectance in space as the indicator of spectral diversity and then compared CV at different scales ranging from 1 mm² to 1 m² to conventional biodiversity metrics, including species richness, Shannon's index, Simpson's index, phylogenetic species variation, and phylogenetic species evenness. In this study, higher species richness plots generally had higher CV. CV showed higher correlations with Shannon's index and Simpson's index than did species richness alone, indicating evenness contributed to the spectral diversity. Correlations with species richness and Simpson's index were generally higher than with phylogenetic species variation and evenness measured at comparable spatial scales, indicating weaker relationships between spectral diversity and phylogenetic diversity metrics than with species diversity metrics. High resolution imaging spectrometer data (1 mm² pixels) showed the highest sensitivity to diversity level. With decreasing spatial resolution, the difference in CV between diversity levels decreased and greatly reduced the optical detectability of biodiversity. The optimal pixel size for distinguishing α diversity in these prairie plots appeared to be around 1 mm to 10 cm, a spatial scale similar to the size of an individual herbaceous plant. These results indicate a strong scale-dependence of the spectral diversity-biodiversity relationships, with spectral diversity best able to detect a combination of species richness and evenness, and more weakly detecting phylogenetic diversity. These findings can be used to guide airborne studies of biodiversity and develop more effective large-scale biodiversity sampling methods.

Key words: biodiversity; Cedar Creek; imaging spectroscopy; remote sensing; scaling; spectral diversity.

INTRODUCTION

Biodiversity loss, one of the most crucial challenges of our time, endangers ecosystem services that maintain human wellbeing (Magurran and Dornelas 2010). “Essential biodiversity variables” have been proposed by ecologists to monitor the variation of biodiversity globally (Pereira et al. 2013). Traditional methods of measuring biodiversity require extensive and costly field sampling by biologists with considerable experience in species identification, and the results may vary with

sampling effort (Gotelli and Colwell 2001, Bonar et al. 2010). It is impossible to acquire sufficient information about changing species distributions through time from field campaigns alone (Heywood 1995). Remote sensing has the potential to detect plant biodiversity and can provide efficient and cost-effective means to determine plant and ecosystem diversity over large areas (Nagendra 2001). Consistent and repeatable remote sensing measurement is critical to long term global biodiversity assessment (Turner 2014).

Diversity can be defined by a large range of indices according to the scale of observation (Whittaker 1960, 1972). Alpha (α) diversity is diversity within a defined place or a habitat at a local scale, typically within a single circumscribed community or field plot; beta (β) diversity

Manuscript received 17 January 2017; revised 12 May 2017; accepted 26 May 2017. Corresponding Editor: David S. Schimel.

⁶E-mail: rw6@ualberta.ca

describes the variation among habitats or communities; gamma (γ) diversity is the total diversity of a large region (landscape, ecoregion, or biome). Local-scale (α) diversity can be measured several ways (Gotelli and Colwell 2001, Magurran 2004). Species richness (the number of species at a site) is the oldest and among the most widely used measure of α diversity. Unlike species richness, heterogeneity indices measure “evenness,” or the apparent number of species taking abundance into account rather than simply the absolute number of species in a given area (Peet 1974). Some metrics (e.g., Simpson or Shannon Indices) combine elements of species richness and evenness into a single metric of α diversity (Peet 1974).

Remote sensing of biodiversity

Recent technological advances in remote sensing, including imaging spectroscopy and LiDAR, can provide detailed spectral and structural information to characterize diversity (Asner 2013). An increasing number of studies applying airborne or satellite remote sensing in biodiversity assessment in different ecosystems, e.g., tropical rainforest (Asner et al. 2008, Asner and Martin 2009, Sanchez-Azofeifa et al. 2009, Féret and Asner 2014), prairie grassland (John et al. 2008, Wang et al. 2016a), island vascular plants (Lucas and Carter 2008), and Arctic regions (Gould 2000). But there is still no single, universally accepted scale or method for remotely sensing biodiversity, and a wide variety of approaches to biodiversity assessment are used, along with multiple definitions of biodiversity (Rocchini 2007, Féret and Asner 2014, Dahlin 2016).

Spectral diversity hypothesis

“Spectral diversity,” sometimes called “optical diversity” (Ustin and Gamon 2010), refers to variation in remote sensing measurements, typically spectral reflectance, across sets of pixels and has been proposed to relate to conventional metrics of biodiversity. Instead of mapping species per se, spectral diversity presumably detects functional and structural properties, which vary among species or functional groups (“optical types”; Gamon 2008, Ustin and Gamon 2010). According to the spectral diversity hypothesis, varying plant leaf traits, canopy structure and phenology can cause wavelength-dependent variations in optical signals (Ustin and Gamon 2010). Since leaf traits (Wright et al. 2004) and canopy structure (Field 1991, Díaz et al. 2015) reflect different evolutionary solutions to resource limitations, spectral diversity can detect different environmental adaptations or resource use strategies. If optical type is regarded as a fundamental vegetation property, resulting from “ecological rules” driven by resource allocation (Field 1991), there should be predictable relationships among plant traits and plant spectral properties.

Recent attempts to assess leaf and canopy functional properties through remote sensing illustrate the promise

of optical approaches to biodiversity assessment. Airborne spectra have been successfully related to plant leaf chemical properties in tropical forests (Asner and Martin 2009, Féret and Asner 2014). Moreover, particular leaf traits can affect canopy level architecture, which can accentuate the leaf spectral properties through multiple scattering and contrasting illumination (Ollinger 2011). As a consequence, variation in leaf- and canopy-scale optical properties and their associated traits in time and space might enable us to detect functional diversity and also biodiversity at different scales.

Scale in ecology and remote sensing

Changing scale alters the perceived patterns of reality, thus changing our understanding of the dynamics of an environmental system (Marceau and Hay 1999). Here, we confine our discussion of scale to the spatial domain, and briefly recognize that other domains are also relevant. In ecology, the concept of scale defines the grain size and spatial extent at which a variety of ecological processes may occur in a landscape (Turner et al. 1989). Scaling up (sampling at coarser scales) changes the level of observed organization and leads to information loss (O’Neill and King 1998). In remote sensing, spatial scale refers to the terms “resolution” (pixel size, determined by sensor technology and flight characteristics) and “spatial extent” (the total area measured). Scale can also relate to spectral scale, the wavelengths (spacing, bandwidth, and spectral range) of spectral bands as measured by a sensor (Marceau and Hay 1999, Rocchini 2007). In addition, temporal scale (frequency and timespan of observation) is important in both ecology and remote sensing, affecting our ability to detect the important processes at the appropriate times.

Meaningful scaling studies in remote sensing are challenging because most campaigns collect data at a single resolution and extent determined by the instrument and sampling platform. Similarly, most ecological sampling methods and the associated definitions are restricted to a particular spatial scale, usually determined by what is possible to sample in a field campaign. Although studies have evaluated sampling effects at large scales (several meters to hundreds meters; Rocchini 2007, Oldeland et al. 2010), few, if any, experimental studies have been done to systematically explore the scale dependence of the spectral-diversity–biodiversity relationship. Consequently, we do not know the “correct” or “ideal” spatial scale for detecting a specific type of diversity (e.g., α or β diversity, species richness, or heterogeneity indices). In remote sensing, practical limitations (trade-offs between sampling resolution and signal-to-noise) result in operational decisions that are largely based on engineering choices in the design of sensors, and these rarely consider the “optimal” design for a biological objective such as assessing biodiversity. The application of current (Turner et al. 2015) or future (Jetz et al. 2016) satellite data to global biodiversity conservation has been

proposed, yet these studies lack a clear discussion of the appropriate or optimal spatial scales for this task. A meaningful evaluation and definition of scale is essential to implementing a biodiversity assessment campaign using remote sensing.

To address these issues, we studied the scale-dependence of spectral diversity in a prairie ecosystem experiment at Cedar Creek Ecosystem Science Reserve (CCESR), Minnesota, USA. We conducted a scaling experiment comparing airborne imagery with ground-based data collected along transects within manipulated plant diversity treatments. Hyperspectral data were collected using several instruments on both ground and airborne platforms, and ground-based images were resampled at several spatial scales to simulate progressively coarse pixel sizes. We used the coefficient of variation (CV) of spectral reflectance in space, which in this case means CV calculated across all pixels in a plot, as the indicator of spectral diversity. We then compared the spectral diversity measured at different scales (pixels) ranging from 1 mm² to 1 m² to various standard metrics of α diversity to investigate how those conventional diversity metrics relate to remote sensing and to explore the scale dependence of spectral diversity.

METHODS

Field site and study design

This study was conducted within the BioDIV experiment at the Cedar Creek Ecosystem Science Reserve, Minnesota, USA (45.4086° N, 93.2008° W). The BioDIV experiment has maintained 168 planted prairie plots (9 × 9 m) since 1994 with species richness of vascular plants ranging from 1 to 16 (Tilman 1997). The species planted in each plot were originally randomly selected from a pool of 18 species typical of Midwestern prairie, including C₃ and C₄ grasses, legumes, forbs, and trees. Of the original 168 plots, 33 plots with species richness ranging from 1 to 16 were selected for this study. These 33 plots included nine monocultures and six replicates of every other richness level (2, 4, 8, and 16) but with differing species combinations (see Appendix S1: Tables S1 and S2).

Imaging spectrometry at fine scale

In the 33 selected plots, an imaging spectrometer (Headwall E Series, Headwall Photonics, Fitchburg, Massachusetts, USA) was mounted on a tram system (Gamon et al. 2006) to collect fine-scale images of the northernmost row of each sampling plot at peak season, both in 2014 (14 plots were sampled from 23 July to 31 July) and 2015 (19 plots were sampled from 17 July to 26 July; Fig. 1a). A speed control circuit was added to the tram cart to maintain a slow and constant moving speed, creating high-fidelity images. The cart speed (0.0256 m/s) allowed us to build clear, high signal-to-noise ratio (SNR)

hyperspectral images under low wind-speed conditions. Typically, wind can affect the field reflectance measurements, especially in canopies with a high vertical structure (Lord et al. 1985). Excessive plant sway caused by strong wind can blur the image, which will degrade the spatial resolution in subsequent analysis. To reduce wind artifacts on windy days, a wind screen consisting of black cloth was placed on two or three sides of the sampling plot, at least 1 m from the sampling area. Data were manually evaluated to further remove any windy (blurred) images.

The imaging spectrometer provided hyperspectral images with a 3-nm spectral resolution (full width at half maximum, FWHM) and a 0.65-nm spectral sampling interval over the 400–1,000 nm range. The focal length of the lens was 17 mm with a field of view (FOV) of ~34°. The spectrometer was mounted 3 m above ground surface, obtaining a ground pixel size of approximately 1 mm² (Fig. 1a). The dimension of the raw image was 1,600 × 1,000 pixels (Fig. 1b). Subsequent image processing avoided 1 m from either end of the plot, and removed 600 pixels from the north side to minimize edge effects, yielding a final image size of 1 × 1 m (Fig. 1b). Reflectance spectra (Fig. 1c) were then extracted from each 1 × 1 m image and used for spectral diversity calculations.

A dark file (DN_{dark,λ}) was obtained before each measurement by covering the lens of the spectrometer with a black lens cap. Scans of a white reference calibration panel (Spectralon, Labsphere, North Sutton, New Hampshire, USA) were taken before and after ground target measurements to calculate surface reflectance. The relative reflectance (ρ) at each wavelength (λ) was calculated as

$$\rho_{\lambda} = \frac{DN_{\text{target},\lambda} - DN_{\text{dark},\lambda}}{DN_{\text{panel},\lambda} - DN_{\text{dark},\lambda}} \quad (1)$$

In this equation, DN_{target,λ} and DN_{panel,λ} indicate the digital number measured at each wavelength (λ , in nm) over the ground target and white reference panel, respectively. All the images were collected under sunny conditions, and reference panel data were collected under similar sky conditions as the target data.

Image resampling

To simulate different spatial scales, a resampling strategy was used to increase the 1 × 1 mm pixels to successively larger spatial scales: 1 × 1 cm, 10 × 10 cm, 25 × 25 cm, 50 × 50 cm, and 1 × 1 m by averaging all the small pixel reflectance values in each “large” pixel. This method assumes an idealized square-wave response on the part of the sensor, ignoring effects from neighboring pixels (Woodcock and Strahler 1987). This scaling up process can also smooth the data, which increases the signal to noise ratio (SNR) of the image, but this effect was ultimately found to be small compared to the treatment effects driven by different diversity levels (see Appendix S1: Fig. S1). To validate this approach, we also

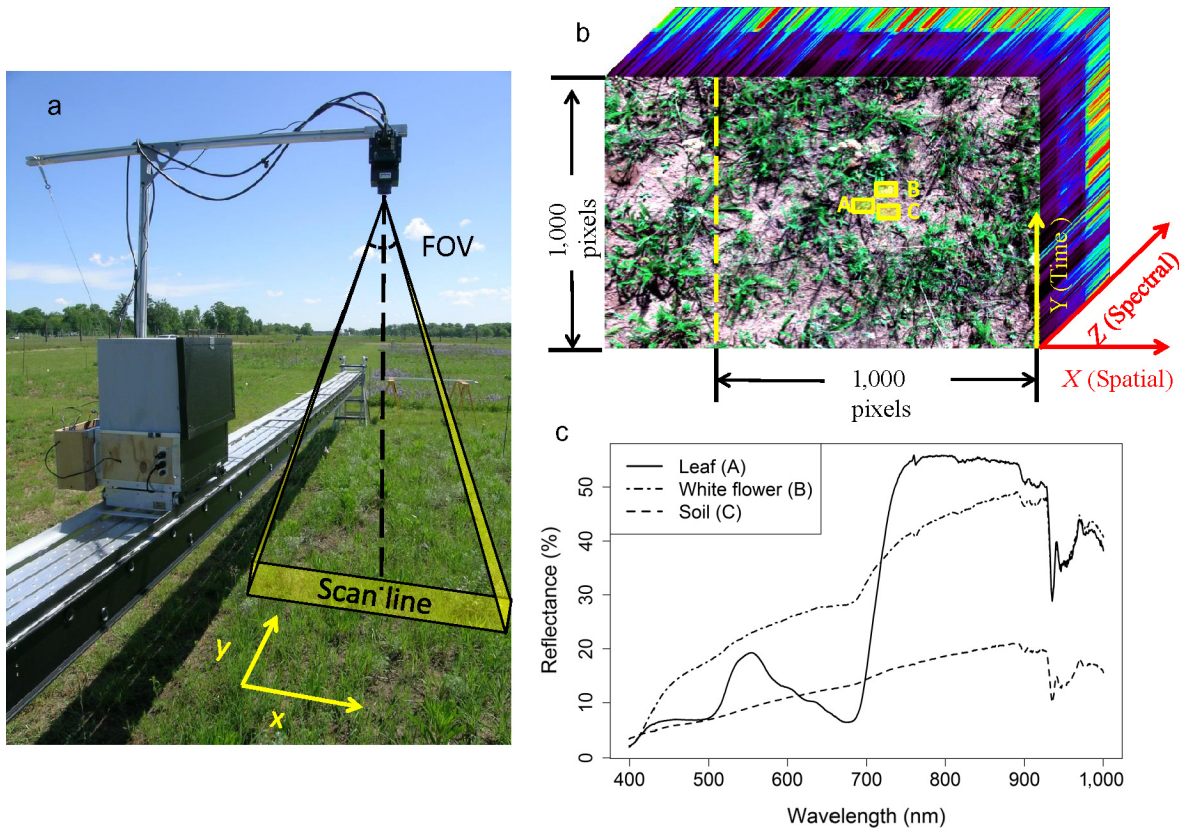


FIG. 1. (a) Headwall imaging spectrometer on the tram. Cart motion along the y -axis produced an image cube. FOV, field of view. (b) Sample image cube from Plot 11, richness = 1 (*Achillea millefolium*). (c) Sample spectra. For each image, 600 pixels of each scan line to the left of the dashed line in panel b were removed from the original image, leaving a $1,000 \times 1,000$ mm square image cube for further analysis. Three yellow squares (A, B, and C) in panel b indicated the positions of the different sunlit targets (leaves, white flowers, and soil) in panel c. Approximately 100 pixels were used to generate each spectrum in panel c.

compared these simulated data to independent samples collected both from the ground and from aircraft at larger (1×1 m) spatial scales.

Whole plot canopy reflectance sampling

To sample entire plots, we measured canopy reflectance of the 33 plots using a non-imaging spectrometer (Unispec DC, PP Systems, Amesbury, Massachusetts, USA) on a tram system (Gamon et al. 2006) at peak season (23 July–3 August 2014). This system allowed a systematic measurement of each 1-m^2 portion of each plot (Wang et al. 2016b). This resulted in a total of 81 measurements (9×9 m) for each plot with approximately 1 m^2 spatial resolution, creating a synthetic image that provided a full sample of each of the 31 plots, and providing one set of independent samples for comparison with the data from the imaging spectrometer on the tram. Edge pixels were discarded to avoid possible edge effects, resulting in a final analysis based on a 7×7 m pixel array. All measurements were made ± 2 h of solar noon to reduce the effects of sun position.

In this whole-plot sampling, both upwelling radiance and down-welling irradiance were measured over the vegetation target and a white reference calibration panel (Spectralon, Labsphere, North Sutton, New Hampshire, USA) that was used to correct for the atmospheric variation and calculate surface reflectance. The relative reflectance (ρ) at wavelength (λ) was calculated as

$$\rho_{\lambda} = \frac{(L_{\text{target},\lambda}/E_{\text{target},\lambda})}{(L_{\text{panel},\lambda}/E_{\text{panel},\lambda})} \quad (2)$$

In this equation, $L_{\text{target},\lambda}$ indicates the radiance measured at each wavelength (λ , in nm) by a downward-pointed detector sampling the surface (“target”), while $E_{\text{target},\lambda}$ indicates the irradiance measured simultaneously by an upward-looking detector sampling the downwelling radiation. $L_{\text{panel},\lambda}$ indicates the radiance measured by a downward-pointed detector sampling the calibration panel (Spectralon, Labsphere, North Sutton, New Hampshire, USA), and $E_{\text{panel},\lambda}$ indicates the irradiance measured simultaneously by an upward-pointed detector sampling the downwelling radiation.

Airborne reflectance sampling

Airborne data for the Cedar Creek region were collected on 2 August 2014 using an imaging spectrometer (AISA Eagle, Specim, Oulu, Finland) mounted on a fixed-wing aircraft (Piper Saratoga, Piper Aircraft, Vero Beach, Florida, USA) operated by the University of Nebraska Center for Advanced Land Management Information Technologies (CALMIT) Hyperspectral Airborne Monitoring Program (CHAMP). Images were collected from a height of 1,540 m and a speed of 196 km/h. The ground pixel size was approximately 1 m². The imaging spectrometer provided 400–970 nm hyperspectral images with 3.3 nm spectral resolution (FWHM). Spectral binning (approximately 10 nm) was used to increase signal-to-noise ratio (SNR) of the data. Imagery acquired with this band configuration has 63 bands across the 400–970 nm continuum. Airborne data covered 125 prairie plots in the BioDIV experiment and data for the 33 ground sampling plots were extracted. This method yielded an image from each plot comparable in scale to the whole-plot canopy reflectance sampling.

To extract reflectance from airborne data, lab-measured calibration coefficients were used to radiometrically convert DN to radiance (W·m⁻²·Sr⁻¹·nm⁻¹). Geometric correction utilized the position and rotational attributes (pitch, roll, and yaw) of the airplane collected by an inflight GPS and inertial measurement unit (IMU; C-Migits III, Systron Donner Inertial, Concord, California, USA) during the flight. Fast Line-of-sight Atmospheric Analysis of Hypercubes (FLAASH) embedded in ENVI version 4.8 (Exelis Visual Information Solutions, Boulder, Colorado) was used for atmospheric correction to convert radiance to reflectance. To obtain a corrected surface reflectance, we used field spectrometer (ASD Field Spec, Analytical Spectral Devices, Inc., Boulder, Colorado, USA) measurements from three 9 × 9 m calibration targets (white, charcoal, and black) made from polyester fabric (Odyssey, J. Ennis, Edmonton, Alberta, Canada) located in the scene to compute coefficients and apply an empirical line correction (Conel et al. 1987) to remove remaining errors in the atmospheric correction.

Comparisons of spectral range

To evaluate the effect of spectral range on the assessment of spectral diversity, we also made measurements with a full-range spectrometer (PSR 3500; Spectral Evolution, Lawrence, Massachusetts, USA). Since these tests found no added benefit of a full-range spectrometer to the method described here, and since they covered a different spectral range from all other instruments, the results of these full-range tests are briefly summarized in Appendix S1: Table S3.

Spectral diversity

As an indicator of spectral diversity of each plot, we used the average coefficient of variation (CV; Wang et al. 2016a), calculated as the average CV for each wavelength from 430 to 925 nm (758 bands in total)

$$CV_{\text{image}} = \frac{\sum_{\lambda=430}^{925} \left(\frac{\sigma(\rho_{\lambda})}{\mu(\rho_{\lambda})} \right)}{\text{number of bands}} \quad (3)$$

where ρ_{λ} denotes the reflectance at wavelength λ and $\sigma(\rho_{\lambda})$ and $\mu(\rho_{\lambda})$ indicate the standard deviation and mean value of reflectance at wavelength λ across all the pixels in one plot, respectively. We calculated CV for all reflectance data, including the tram images, synthetic images using ground canopy reflectance and airborne images. In this case, CV expresses the spectral heterogeneity among pixels with one single value per plot. Sample CV spectra and the spectral averaging method are illustrated in Fig. 2 for two plots of contrasting diversity. (Note that for spectral range tests, CV was calculated over different spectral ranges, as described in results and Appendix S1: Table S3.)

Conventional diversity metrics

To calculate diversity metrics based on richness and evenness, biomass data were collected from all plots. Aboveground living plant biomass of the selected 33 plots was measured in late July to early August (4 August 2014 and 27 July–3 August 2015). Plots were sampled by clipping, drying, and weighing four parallel and evenly spaced 0.1 × 6 m strips per plot. The biomass of each strip was sorted to species. Planted species richness was the number of species originally planted

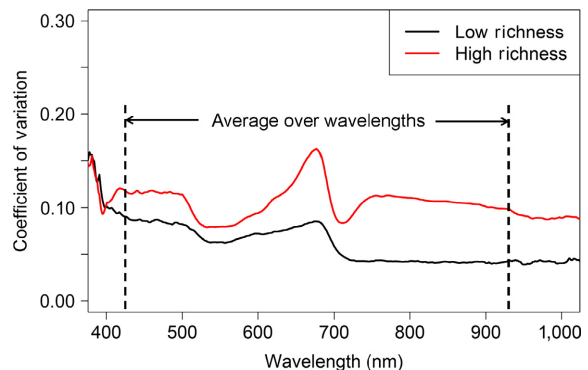


FIG. 2. Sample coefficient of variation (CV) spectra of plots with different species richness levels (1 and 16). As a summary metric, an average CV was calculated over 430–925 nm as indicated in Eq. 3 and Fig. 1. Data were derived from the Headwall E Series imaging spectrometer sampling at 1 mm pixels for plots 11 and 34 (See Appendix S1: Tables S1 and S2 for detailed descriptions of sampling plots).

TABLE 1. Summary of diversity metrics used in this study where p_i is biomass proportion of the i th species.

Diversity metric	Description/Equation
Planted species richness, S_0	Number of species originally planted and subsequently maintained in each plot.
Observed species richness, S	Number of harvested species in each plot (includes rare species).
Shannon's index, H'	$H' = -\sum p_i \times \ln(p_i)$
Simpson's index, D	$D = 1/\sum p_i^2$
Evenness, J'	$J' = H'/\ln(S)$
Phylogenetic species variability, PSV	PSV varies between 0 and 1. Values close to 1 have higher phylogenetic diversity.
Phylogenetic species evenness, PSE	PSE varies between 0 and 1. Values closer to 1 have higher phylogenetic diversity and evenness.

and maintained in each plot, providing a nominal metric of biodiversity. In most cases the observed species number and richness derived from harvested vegetation varied from the planted species number and richness due to missing species or other species present in the plot besides the ones maintained. As a result of the periodic weeding, the abundance of these non-maintained species was typically much less than the maintained species, allowing us to assume that the planted plant species richness provided a reasonable approximation of the observed species richness.

Previous results (Wang et al. 2016a) have suggested that spectral diversity may be affected by evenness as well as species richness. Consequently, we also calculated three indices that weighted species abundance by proportional biomass, thus accounting for the effects of rare or common occurrences (Shannon's index [Shannon 1948]), the reciprocal of Simpson's index [Simpson 1949, Williams 1964], and species evenness [Pielou 1966]; Table 1) and related these metrics to spectral diversity (CV) at different scales. Shannon's index expresses the equitability of all the species while Simpson's index focuses on a few dominant species (Whittaker 1972).

Phylogenetic diversity is recognized as representing an integrated measure of functional differences among species and often helps explain ecological variation among species beyond what can be explained by richness alone (Cadotte et al. 2008, 2009, Cavender-Bares et al. 2009, Srivastava et al. 2012). However, metrics of phylogenetic diversity that rely on total evolutionary distances among species in an assemblage are strongly associated with species richness. We intentionally chose metrics of phylogenetic diversity independent of species richness to separate variation associated with species richness from that associated with evolutionary distinctiveness of species in assemblages. Phylogenetic data was based on the phylogeny from Zanne et al. (2014) and pruned to include only the species observed in BioDIV. To study the influence of phylogenetic diversity on spectral diversity, two indices independent of species richness, phylogenetic species variability (PSV) and phylogenetic species evenness (PSE) (Helmus et al. 2007), were calculated with the picante R package (Kembel et al. 2010). PSV quantifies how phylogenetic relatedness decreases the variance of a hypothetical neutral trait shared by all species in a

community. PSV is directly related to mean phylogenetic distance and ranges from 0 (low) to 1 (high) and compares observed phylogenetic distinctness to null communities. PSE is PSV modified to incorporate relative species abundance. The maximum attainable value of PSE (i.e., 1) occurs when each species has the same abundance and evolves independently from a common starting point (Helmus et al. 2007). In this case, PSE was weighted by biomass at the plot level.

RESULTS

Effect of spatial scale

The mean reflectance of each image was the same across spatial scales, but the variation around this mean (expressed as SD and max/min in Fig. 3, and as the CV in subsequent figures) decreased with increasing pixel size, revealing the sensitivity of the spectral-diversity–species-richness (SR) relationship to pixel size.

Spectral diversity (measured by CV) increased with planted species richness. Increasing pixel size reduced the sensitivity of spectral diversity to planted species richness (Fig. 4a). By 10×10 cm and above, the linear relationship between CV and planted species richness started to disappear, and the relationships were no longer significant at $P = 0.05$ for pixel sizes above 10×10 cm. When applying an analysis of covariance (ANCOVA) test to see whether the regression slopes varied with scales, there was no significant difference between slopes of regression at 1 mm and 1 cm scales, but the difference of slopes between 1 cm and 10 cm was significant ($P = 0.009$).

There was no significant relationship found between observed species richness and spectral diversity (Fig. 4b). The relationship between CV and Shannon's index (Fig. 4c) was similar to the CV-planted species richness relationship (Fig. 4a). Simpson's index (Fig. 4d) showed stronger relationships with spectral diversity than species richness and Shannon's index. The relationships between CV and Shannon's index and Simpson's index also weakened with increasing pixel size. The CV–Simpson's-index relationship was still maintained even at coarse spatial scales (at least better than the other comparisons with observed species richness, planted species richness, and

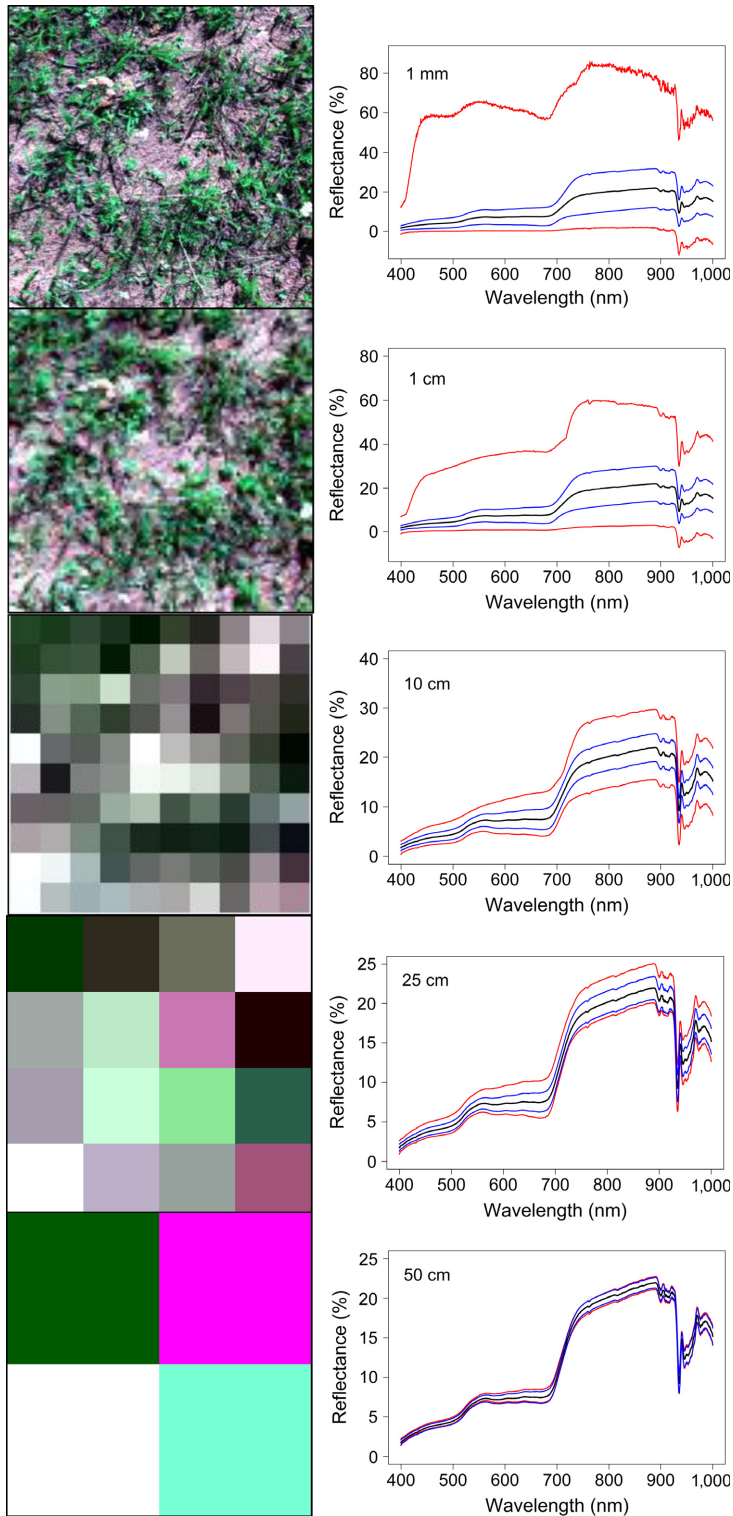


FIG. 3. Sample images and reflectance spectra at different sampling pixel sizes (1 mm to 50 cm diameter, as indicated in the spectral plots). The image shown here was the second meter from the west of Plot 11 (planted species richness = 1; See Appendix S1: Tables S1 and S2 for detailed descriptions of sampling plots). The dimension of the original image in the top panel was $1,000 \times 1,000$ mm pixels (approximately 1×1 m), which was successively degraded by resampling to progressively larger sizes (up to 50×50 cm in the bottom panel). Colored lines indicate mean (black), standard deviation (blue), and min/max (red) reflectance. The images on the left were stretched to maintain contrast and the spectral plots on the right showed the true contrast.

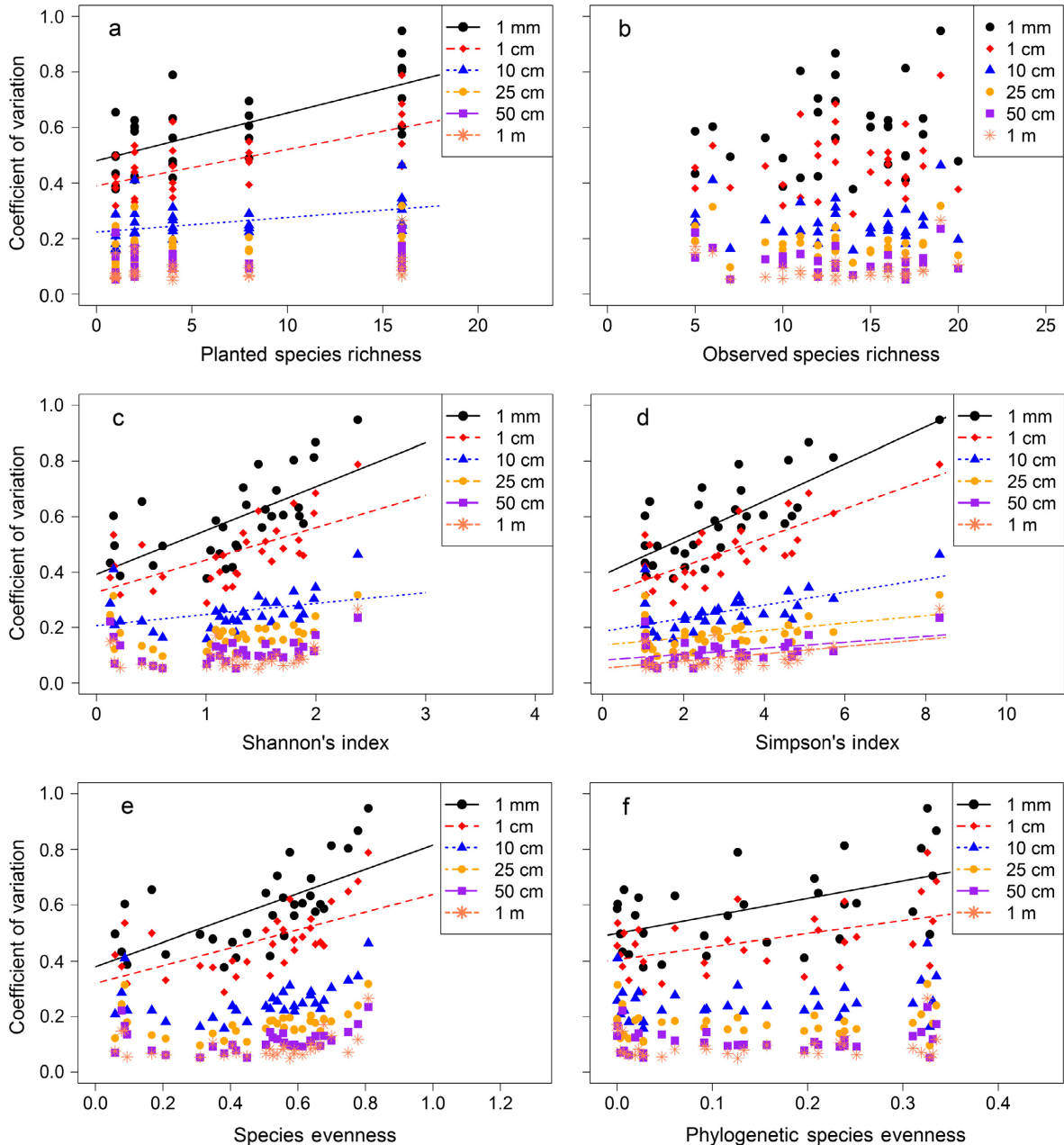


FIG. 4. Spectral diversity (coefficient of variation) vs. conventional biodiversity metrics ((a) planted species richness, (b) observed species richness, (c) Shannon's index, (d) Simpson's index, (e) species evenness, (f) phylogenetic species evenness) for varying pixel sizes (diameters). The definitions of conventional biodiversity metrics are in Table 1. Fit lines are not shown for $P > 0.05$.

Shannon's index). For both Shannon's index and Simpson's index, the difference between regression slopes at 1 mm and 1 cm scales were not significant. There were significant differences between slopes at larger scales ($P < 0.001$).

Evenness (Fig. 4e) showed similar but slightly weaker relationship with spectral diversity than Shannon's index. A linear relationship was found between phylogenetic

evenness (Fig. 4f) and spectral diversity at fine scales (1 mm). The relationship was not as strong as the species-evenness-spectral-diversity relationship but still significant at small spatial scales. Similar to the CV-plant-species-richness relationships, ANCOVA tests suggested no significant difference between 1 mm and 1 cm regression slopes for CV-species-evenness and CV-phylogenetic-evenness relationships.

Key results from Fig. 4 were summarized in Table 2. For all diversity metrics, the difference in CV between diversity levels tended to decrease with increasing pixel size. For most biodiversity metrics, at a resolution of 10×10 cm or higher, much of the power to assess biodiversity was lost. At 1 m resolution, there was very little power to distinguish diversity levels for most metrics of biodiversity. Only CV–Simpson’s-index maintained significant relationships at all spatial scales (Table 2).

Effect of wavelength regions

To investigate spectral scale, we examined the CV from different spectral regions. The relative contribution to CV varied by wavelength. CV spectra at different pixel sizes showed that, at a fine scale (pixel size < 25 cm), high richness plots had a higher average CV than low richness plots. This pattern was apparent for all wavelengths but was especially strong for the visible region (Fig. 5). By contrast, the relative importance of the NIR increased as spatial scale increased. At scales of 10 and 25 cm, it was hard to distinguish richness levels from the visible spectra but the NIR region was still distinguishable. At coarser scales (pixel size > 25 cm), all of the CV spectra overlapped, except for the highest richness level (richness = 16), illustrating the declining power to distinguish richness at coarser spatial scales.

To provide further insight into the spectral regions contributing to spectral diversity information (Fig. 5), we compared the CV calculated over different spectral ranges (430–900 nm), and compared these results to the Simpson’s index, which displayed the strongest correlation with CV (Table 2). We also conducted independent tests over a larger spectral range using a full-range spectrometer. The full range spectrometer did not indicate improved results over the VIS–NIR range (Appendix S1: Table S3). Consequently, in this study, we confined our primary analyses to the VIS–NIR range (the range covered by our imaging spectrometer).

At a fine scale (≤ 25 cm diam.), the CV values in visible wavelengths (430–700 nm, CV_{visible}) were larger than the CV of visible + NIR (430–900 nm, CV_{VN}) and the CV of NIR (700–900 nm, CV_{NIR}) (Fig. 6 and Table 3). Similarly, the R^2 of CV_{visible} –Simpson’s-index was similar to the CV_{VN} –Simpson-index and larger than CV_{NIR} –Simpson’s-index at fine scales. These relationships changed at larger pixel sizes. With increasing pixel size, R^2 of all three regressions decreased, but the R^2 of the CV_{NIR} –Simpson’s-index relationship decreased with resolution less than the other two. Consequently, at the 25- and 50-cm pixel sizes, R^2 of the CV_{NIR} –Simpson’s-index became the largest among the three CV formulations derived from different spectral ranges, and still retained significant correlations ($P < 0.01$). The ANCOVA test indicated significant difference between slopes of CV–Simpson’s-index relationships at different scales ($P < 0.01$ for all of the three spectral regions).

TABLE 2. Slopes of regressions between coefficient of variation (CV) and conventional diversity metrics (see Table 1) at different scales (pixel diameter values).

Pixel diam.	Planted richness	Observed richness	Shannon’s index	Simpson’s index	Evenness	PSV	PSE
1 mm	0.017 (0.467***)	– (0.036NS)	0.158 (0.427***)	0.067 (0.583***)	0.435 (0.421***)	– (6×10^{-4} NS)	0.629 (0.273**)
1 cm	0.013 (0.44***)	– (0.027NS)	0.116 (0.378***)	0.052 (0.571***)	0.317 (0.364***)	– (8×10^{-5} NS)	0.459 (0.237**)
10 cm	0.005 (0.21***)	– (0.003NS)	0.040 (0.131*)	0.024 (0.357***)	– (0.127NS)	– (0.082NS)	– (0.056NS)
25 cm	– (0.11NS)	– (0.046NS)	– (0.041NS)	0.013 (0.185*)	– (0.045NS)	– 8.64×10^{-5} (0.176*)	– (0.126NS)
50 cm	– (0.123NS)	– (0.055NS)	– (0.035NS)	0.011 (0.174*)	– (0.041NS)	– 6.34×10^{-5} (0.134*)	– (0.017NS)
1 m	– (0.086NS)	– (9e–4NS)	– (0.048NS)	0.013 (0.239**)	– (0.054NS)	– (0.078NS)	– (0.016NS)

Notes: Coefficients of determination, R^2 , are shown in parentheses. PSV and PSE indicate the phylogenetic species variability and phylogenetic species evenness, respectively. Dashes indicate that no slope is shown; slopes were shown only for significant relationships ($P < 0.05$). NS 0.05 < P , * 0.01 < P < 0.05, ** 0.001 < P < 0.01, *** P < 0.001.

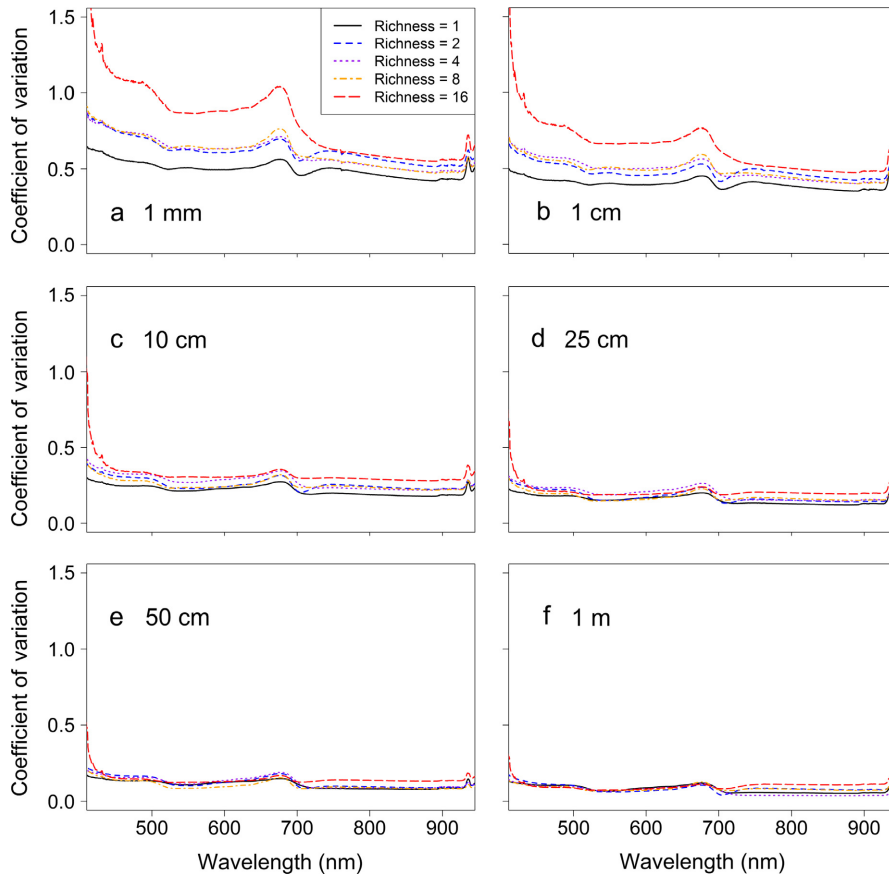


FIG. 5. Coefficient of variation spectra at different pixel sizes resampled from ground-sampled image cubes (imaging spectrometer on the tram) for pixel sizes 1 mm to 1 m. Line color indicates different planted species richness levels.

Comparison of instruments

A comparison of different methods yielded good agreement between instruments and sampling methods. The CV–planted-species-richness relationship in the synthetic images (1-m² pixels) fit the trend found in the resampled images (spanning 1 mm² to 1 m² pixels; Fig. 7). CV values for the different diversity levels were slightly more variable when calculated from the imaging spectrometer on the ground than when calculated from the non-imaging spectrometer or the airborne spectrometer (Fig. 7a). Airborne CV values were slightly smaller than synthetic and ground measurements at all planted species richness levels. Regardless of method, by 1 × 1 m, there was very little power to distinguish planted richness levels except at the most extreme levels of 1 vs. 16 species.

DISCUSSION

Scale dependence of spectral diversity

Applying the imaging spectrometer using the tram system on the experimental biodiversity plots allowed us to

collect very high resolution (1-mm² pixel size) images and test the scale dependence of the spectral-diversity–biodiversity relationship. Instead of enumerating plant species, CV is an abstract expression that represents the information content (variability) of the reflectance spectra among pixels. Using this method, the detectability of biodiversity with remote sensing declined dramatically when scaling up from 1 mm² to 1 m² in this plot-level experiment. The slightly smaller CV value calculated from the airborne image compared to synthetic images (created from the Unispec spectrometer) may be due to a blurring result caused by the point spread function of the airborne imaging spectrometer, which reduced the variation between neighboring pixels. The overall consistency of the patterns across spatial scales for the different methods indicated a strong effect of spatial scale on the ability to detect α biodiversity with optical remote sensing methods.

Observed-diversity–richness–evenness

The stronger relationship between spectral diversity and Simpson's index than between spectral diversity and observed species richness agrees with recent studies

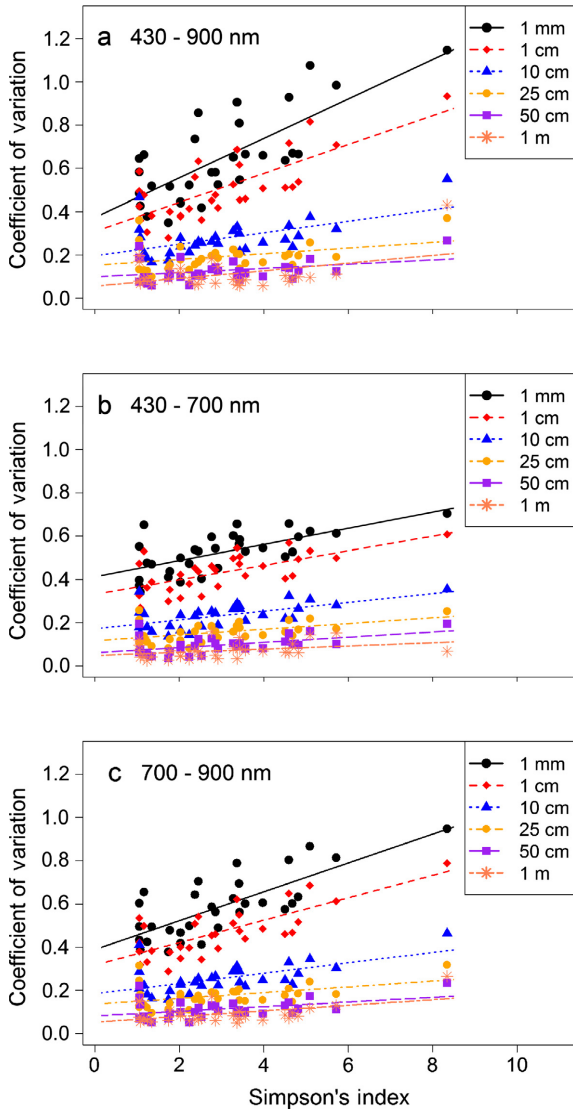


FIG. 6. Spectral diversity (coefficient of variation) vs. Simpson's index for different wavelength regions (a, 430–900 nm; b, 430–700 nm; c, 700–900 nm) and different pixel sizes (1 × 1 mm to 1 × 1 m). Slopes and R^2 of the regressions were listed in Table 2.

(Oldeland et al. 2010, Wang et al. 2016a) that measures of evenness can improve the correlation between spectral diversity and conventional diversity metrics. Integrating species evenness adds additional information on community structure beyond species richness per se. These findings suggest that spectral diversity relates to the heterogeneity within a small region that is determined by a combination of species composition, richness, and evenness.

Both Shannon's index and Simpson's index are commonly used metrics in quantifying elements of biodiversity but the two metrics show variable responses to different combinations of richness and evenness (Nagendra 2002). In our study, spectral diversity showed a stronger relationship with Simpson's index than Shannon's index, which agrees with findings from a study in tropical forests (Schäfer et al. 2016). This may be because Simpson's index is more sensitive to dominant or common species than Shannon's index, which assumes all species are present and randomly sampled (Peet 1974). This Bio-DIV experiment is a highly manipulated experimental landscape, weeded in summer to maintain species richness so that the percentage of rare species is small and the evenness of low richness plots tends to be low. It is also reasonable that planted species richness, which implicitly includes a degree of evenness by ignoring "rare," unintended species (which likely do not contribute much or at all to the optical signals measured here), leads to a better correlation to spectral diversity than observed species richness (which includes more rare species that are not an intended part of the experiment).

Species evenness-phylogenetic evenness

In principle, if phylogenetic diversity reflects functional and phenotypic properties that are detectable with remote sensing, spectral diversity should increase with phylogenetic diversity. The two indices we used were PSV and PSE; the latter metric incorporates abundance, but both are independent of species richness. Both metrics showed significant relationships with CV (Table 2). Similar to the indices at the species level, the significant relationship between CV and PSE at fine spatial scale (1 mm) disappeared rapidly at coarser scales (pixel size > 1 cm). These

TABLE 3. Spectral diversity (coefficient of variation) of different wavelength vs. Simpson's index.

Pixel size	CV _{VN}		CV _{visible}		CV _{NIR}	
	Slope	R ²	Slope	R ²	Slope	R ²
1 mm	0.067	0.583***	0.091	0.567***	0.037	0.437***
1 cm	0.052	0.571***	0.067	0.567***	0.034	0.434***
10 cm	0.024	0.356***	0.027	0.310***	0.020	0.343***
25 cm	0.013	0.185*	0.013	0.129*	0.013	0.229**
50 cm	0.011	0.173*	0.010	0.107NS	0.012	0.244**
1 m	0.013	0.239**	0.018	0.180*	0.007	0.109NS

Notes: CV_{VN}, CV calculated using 430–900 nm reflectance; CV_{visible}, CV calculated using 430–700 nm reflectance; CV_{NIR}, CV calculated using 700–900 nm reflectance.

NS 0.05 < P, * 0.01 < P < 0.05, ** 0.001 < P < 0.01, *** P < 0.001.

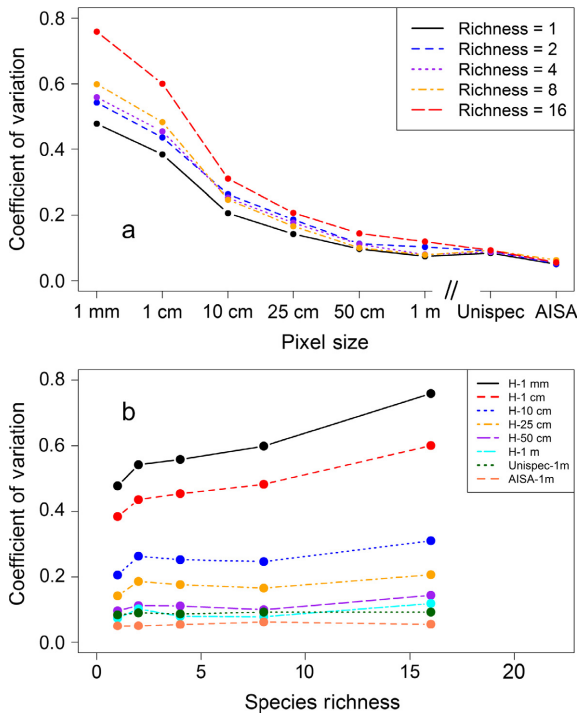


FIG. 7. (a) Coefficient of variation as a function of pixel size for the resampled Headwall images and AISA Eagle airborne data for 125 plots. (b) Comparison of the coefficient-of-variation–planted-species-richness relationship at different scales obtained from different instruments (Headwall [H], UnispecDC [Unispec], and AISA Eagle [AISA]) and platforms (tram and aircraft).

results indicate that species richness measures, particularly when they account for abundance, capture more detectable variation than phylogenetic distinctiveness measures that are independent of species richness. These findings are consistent with recent studies indicating that species richness and evenness are often the most critical factors explaining relationships between biodiversity and ecosystem function (Zhang et al. 2012).

Optimal pixel size

The predictability of a phenomenon is scale-dependent both in ecology (Costanza and Maxwell 1994) and remote sensing (Woodcock and Strahler 1987). In ecology, grain size is the extent of the elementary sampling units and the minimum size of measure (Costanza and Maxwell 1994, Legendre and Legendre 1998). Fine-scale sampling provides more information about detailed patterns that will be lost at coarse scales. In this study, considerable information on fine-scale variability decreased with increasing pixel size, and this result is in accordance with the finding that significant information may be lost when the sampling elements are scattered and small compared to the pixel size (O'Neill et al. 1986). From a remote sensing perspective, the spatial structure of an image relates to the size of the objects in the scene and the spatial resolution

(pixel size). Woodcock and Strahler (1987) noted local variance peaked when the size of the object equaled (or was close to) the spatial resolution of the image, which may help explain our results. In our study, the optimal pixel size for distinguishing diversity levels in these prairie plots, particularly for the visible spectral region (sensitive to leaf pigments) appears to be in the range of 1 mm to 10 cm, a range of spatial scales similar to those of a single leaf or herbaceous plant species in this experimental prairie landscape.

In another study of prairie grassland in southern Alberta, Canada, CV calculated with airborne imagery correlated well with biodiversity metrics, e.g., richness and Shannon's index even at 1-m² scale (Wang et al. 2016a), yet in our study of experimental plots, this correlation was largely lost by 1 m². In experimental plots of constant size with long-term maintenance, grain and extent are determined and perhaps maintained artificially but these properties may be different or exhibit inconstant temporal behavior in real landscapes. The larger extent captured in airborne sampling in a natural landscape can introduce higher-level diversity effects (e.g., β diversity), which may explain contrasting results across studies at different spatial scales or settings. As well, the discontinuity measured on a real landscape may appear continuous when broken into finer grained observations, especially at a small extent (9×9 m) as in this study. When considering other applications of airborne and satellite remote sensing in biodiversity detection in natural landscapes, spectral diversity may reveal variation between species, between dominant species, or even the transition from α diversity to β diversity with increasing grain size and spatial extent. These factors of scale are generally not considered explicitly in remote sensing campaigns addressing biodiversity, most of which do not use experimental approaches, but are restricted to a single grain size and extent.

Considering the surrogacy hypothesis (Magurran 2004), high species richness in one taxon may be related to high richness in other, particularly at higher trophic levels, as has been demonstrated in insect herbivore communities (Siemann et al. 1998, Haddad et al. 2009). High environmental variation, e.g., temperature or topographical, diversity is frequently related to high species richness (environmental surrogacy), such as in the case of habitat heterogeneity and butterfly diversity (Kerr et al. 2001). It is possible that the relationship between spectral diversity and species richness at certain scales is fortuitous and often remains significant at even coarse spatial scales because we actually see something indirectly related to species richness rather than species richness per se. Presumably, species richness is also related to functional diversity to some extent (e.g., Petchey and Gaston 2002, Flynn et al. 2011) despite well-understood complexities (Cadotte et al. 2011, Violle et al. 2012). A more diverse ecosystem is thus likely to include a greater variety of functional behaviors as indicated by plant traits relate to different leaf biochemical content and

canopy structure. The variation in plant traits among species can affect the optical properties of plants and lead to spectrally detectable features (spectral diversity). Our findings suggest that, for pixels much larger than the individual plant size, a direct detection of α diversity is not feasible, although other measures of diversity at larger scales may apply. The results suggest that further assessment of the scale dependence of the spectral-diversity–biodiversity relationships for different vegetation types (e.g., different crown sizes) is warranted, particularly if the goal is to develop reliable and repeatable remote methods of assessing biodiversity. We recommend that similar scaling studies be conducted in natural landscapes to better reveal both the underlying causes and larger significance of the scale-dependent relationships reported in this study. Such studies should also address much larger pixel sizes, such as are proposed for spaceborne sensors, and should enable fully testing the degree to which regional α and β diversity are detectable for grain sizes that are relatively coarse when compared to those used in this study.

The ecological concept of patch size is clearly relevant to the remote sensing of spectral diversity. Broadly, a patch can be defined as a relatively homogeneous spatial unit that is different from its neighbors in nature or appearance (Wu and Loucks 1995, Bazzaz 1996). Variation within a patch is influenced by the minimum size of all of the patches that will be mapped as well as which components of the system are ecologically relevant to the organism or process of interest. In this study, we used visible to near-infrared waveband regions to calculate the coefficient of variation and the optical “patch size” appeared to vary slightly with spectral region. The different responses of visible and near-infrared spectral regions to pixel size suggested possible changes in the relative contribution to spectral diversity from leaf traits to canopy structure with increasing pixel size. Some leaf traits (e.g., pigment levels) are detectable in the visible region (Ollinger 2011, Ustin 2013), and the sensitivity of CV_{vis} to planted species richness or Simpson’s index was quickly lost at pixel sizes above that of the individual leaves and plants. In this case, the relevant “patch size” seems close to that of an individual leaf or plant. On the other hand, the NIR region is sensitive to canopy structure (Ollinger 2011, Ustin 2013), and the CV_{NIR} –Simpson’s-index retained a significant correlation at relatively large spatial scales (25–50 cm), suggesting the relevant “patch size” of canopy structure is larger than that of leaf traits.

Spectral resolution and range also affect the spectral-diversity–biodiversity relationship. When compared to multispectral data, adding spectral information has been shown to increase the accuracy of biodiversity estimation (Rocchini 2007). Using full range spectra including the shortwave infrared (400–2,500 nm) could add information on other biochemical properties, e.g., leaf water content, pigment, nitrogen content, and lignin (Asner and Martin 2009). While not easily possible in this study due to the limited range of our primary instruments, future studies

should consider the effects of the full spectral range on the scale dependence of the spectral diversity–biodiversity relationship. In our initial tests (Appendix S1: Table S3), sampling the full spectral range did not enhance the CV–Simpson’s-index relationships over the VIS–NIR range, but given the wide range of vegetation types and possible analytical approaches not considered here, these negative findings should not be viewed as conclusive. We note that many of the promising applications of full-range spectroscopy to biodiversity have been developed for tropical forests, which are functionally (and spectrally) distinct from the prairie species studied here. Full-range spectroscopy can be very useful in assessing leaf and plant traits (Asner and Martin 2009), and presumably would be useful in studying other aspects of diversity (e.g., functional diversity) not considered here. Consequently, further studies of spectral range for biodiversity assessment are needed, and these studies should consider more than one biome type, and additional aspects of diversity in addition to the ones considered here.

Finally, hierarchy theory suggests that the scale of measurement limits the scope of what can be captured in an observation (Ahl and Allen 1996). The scaling effect of observation relies on the observer’s choice of measurement. Here, we would expect that the “best” pixel size may vary among biomes and communities having different dominant species, e.g., prairie (with small plant sizes) vs. forests (where tree crown size is typically several meters in diameter). As well, for natural landscapes, there may be higher-level effects at coarser spatial scales that reflect other aspects of diversity besides α diversity, e.g., β diversity as driven by environmental gradients or disturbance.

Confounding effects

The CV–diversity relationship may depend on the stand structure, including plant density and spacing, homogeneity of distribution among the species, and the presence of non-vegetated cover (e.g., bare soil). In this system, plant density is known to depend on diversity, which is maintained by weeding; as a consequence, lower diversity plots are less densely vegetated, have more bare ground, and have been shown to be more invasible (Naeem et al. 2000). As diversity declines and plant density in the plot decreases, spectral diversity is impacted (revealed as increased CV values for low diversity plots) and the degree of cover and bare soil affected the ability to detect α diversity. In a separate modeling analysis (data not shown), adding soil spectra to pure plant pixels increased plot-level CV and weakened the spectral-diversity–biodiversity relationships but the spectral-diversity–biodiversity relationships stayed significant. Clearly, more work on the effects of stand structure including the influence of bare soil and other non-vegetated cover types on the CV–diversity relationship is needed, and this is the focus of current studies (in preparation). Forest diversity experiments in which plant stem density is held constant while species richness and

phylogenetic diversity vary are a means to uncouple density and diversity in manipulated experimental systems and could be considered in future experimental studies of biodiversity from remote sensing.

CV shows potential in estimating biodiversity using remote sensing, and is not very sensitive to the sample size (Appendix S1: Figs. S2 and S3). But CV condensed the information contained in a full spectrum into a single value, which may not fully use the entire spectral information available with other methods. Particularly for assessing functional diversity tied to plant traits or biochemical composition, full spectral information can be critical. Other spectral diversity methods have been proposed to calculate diversity metrics in the principal components (PC) space, e.g., mean distance from the centroid of all PCs (Rocchini 2007, Oldeland et al. 2010), or to sum of the variance and convex hull volume for the first three PCs (Dahlin 2016). Future studies should compare the performance of different spectral diversity metrics across spatial, temporal, and spectral scales.

CONCLUSION

The scale dependence of processes and patterns are central topics in both ecology and remote sensing. Few studies have considered the scale dependence of spectral diversity due to the difficulty of obtaining comparable remote sensing data at different scales. To address this challenge, we developed a method to apply imaging spectrometry at multiple spatial resolutions using an imaging spectrometer mounted on a ground-based tram system in a manipulated experiment. We compared these results to other ground sampling and airborne methods to investigate the spectral-diversity–biodiversity relationship at different grain sizes (pixel sizes). Among the conventional biodiversity indices that we tested, spectral diversity showed the strongest relationship with Simpson's index, likely because Simpson's index combined species richness and evenness and was sensitive to dominant species. Our fine-scale study also showed rapid information loss with increasing pixel size; the best resolution to detect α diversity using spectral diversity was the size close to a typical herbaceous plant leaf or single canopy. Although it will become more complicated as the dimensionality of number of species, and their identity increases, most likely, the "optimal" pixel size for detecting plant biodiversity with this method would vary depending upon the size of the individual organisms in question, and more work across a variety of ecosystems is needed to test this hypothesis.

While restricted to ground and airborne sampling, our study provides insights for the design and application of future spaceborne and airborne sensors, and suggests that direct assessment of α diversity, at least for prairie regions, may require spatial resolution higher than most existing satellite sensors. These findings can be exploited in future airborne remote sensing campaigns to determine the most appropriate pixel size for spatially

extensive assessment of α diversity. It is also critical to understand the scale dependence of the spectral diversity–biodiversity relationship as we transit from manipulated experiments to natural landscapes; natural landscapes may differ in their spectral patterns due to contrasting patch sizes, as a result of vegetation clumping (e.g., due to vegetative reproduction, clonality, or dispersal limitation), which influence the grain size and spatial extent optimal for detection of biodiversity. Further studies in natural landscapes are also needed to explore higher-level (e.g., β diversity) effects on spectral diversity, which may be more amenable to remote sensing. Data from multiple ecosystems and vegetation types, e.g., prairie and forest, should be included in future studies, with attention to the consequences of canopy and patch size on the scale dependence of the biodiversity–spectral-diversity relationship.

ACKNOWLEDGMENTS

We thank staff at the Cedar Creek Ecosystem Science Reserve, particularly Troy Mielke and Kally Worm. We thank Rick Perk and Abby Stilwell from CALMIT, University of Nebraska-Lincoln for acquiring and processing airborne data. We also thank Aidan Mazur and Melanie Sinnen from University of Wisconsin-Madison for helping collect the whole-plot reflectance data. We appreciate Anna Schweiger from University of Minnesota for her coordination of data collection in 2015. This study was supported by a NASA and NSF grant (DEB-1342872) to J. Cavender-Bares, a NSF-LTER grant (DEB-1234162) to J. Cavender-Bares, and by iCORE/AITF (G224150012 & 200700172), NSERC (RGPIN-2015-05129), and CFI (26793) grants to J. Gamon, and a China Scholarship Council fellowship to R. Wang.

LITERATURE CITED

- Ahl, V., and T. F. H. Allen. 1996. *Hierarchy theory: a vision, vocabulary, and epistemology*. Columbia University Press, New York, New York, USA.
- Asner, G. P. 2013. Biological diversity mapping comes of age. *Remote Sensing* 5:374–376.
- Asner, G. P., and R. E. Martin. 2009. Airborne spectrometry: mapping canopy chemical and taxonomic diversity in tropical forests. *Frontiers in Ecology and the Environment* 7:269–276.
- Asner, G. P., et al. 2008. Remote sensing of native and invasive species in Hawaiian forests. *Remote Sensing of Environment* 112:1912–1926.
- Bazzaz, F. A. 1996. *Plants in changing environments: linking physiological, population, and community ecology*. Cambridge University Press, Cambridge, UK.
- Bonar, S., et al. 2010. An overview of sampling issues in species diversity and abundance surveys Pages 376 in A. E. Magurran and B. J. McGill, editors. *Biological diversity: frontiers in measurement and assessment*. Oxford University Press, Oxford, UK.
- Cadotte, M. W., et al. 2008. Evolutionary history and the effect of biodiversity on plant productivity. *Proceedings of the National Academy of Sciences USA* 105:17012–17017.
- Cadotte, M. W., et al. 2009. Using phylogenetic, functional and trait diversity to understand patterns of plant community productivity. *PLoS ONE* 4:1–9.
- Cadotte, M. W., et al. 2011. Beyond species: Functional diversity and the maintenance of ecological processes and services. *Journal of Applied Ecology* 48:1079–1087.

- Cavender-Bares, J., et al. 2009. The merging of community ecology and phylogenetic biology. *Ecology Letters* 12:693–715.
- Conel, J. E., R. O. Green, G. Vane, C. J. Bruegge, R. E. Alley, and B. J. Curtiss. 1987. AIS-2 radiometry and a comparison of methods for the recovery of ground reflectance. *Proceedings of the 3rd Airborne Imaging Spectrometer Data Analysis Workshop/JPL Publ. Volume 87–30*. Pasadena, California. <http://ntrs.nasa.gov/search.jsp?R=19880004375>
- Costanza, R., and T. Maxwell. 1994. Resolution and predictability: An approach to the scaling problem. *Landscape Ecology* 9:47–57.
- Dahlin, K. M. 2016. Spectral diversity area relationships for assessing biodiversity in a wildland–agriculture matrix. *Ecological Applications* 26:2756–2766.
- Díaz, S., et al. 2015. The global spectrum of plant form and function. *Nature* 529:167–171.
- Féret, J.-B., and G. P. Asner. 2014. Mapping tropical forest canopy diversity using high-fidelity imaging spectroscopy. *Ecological Applications* 24:1289–1296.
- Field, C. B. 1991. Ecological scaling of carbon gain to stress and resource availability. Pages 35–65 *in* W. E. Winner, E. J. Pell, and J. Roy, editors. *Response of plants to multiple stresses*. Elsevier Inc
- Flynn, D. F. B., et al. 2011. Functional and phylogenetic diversity as predictors of biodiversity–ecosystem-function relationships. *Ecology* 92:1573–1581.
- Gamon, J. A. 2008. Tropical sensing — opportunities and challenges. Pages 297–304 *in* G. Kalacska and A. Sanchez-Azofeifa, editors. *Hyperspectral remote sensing of tropical and subtropical forests*. CRC Press Taylor & Francis Group, Boca Raton, Florida, USA.
- Gamon, J. A., et al. 2006. A mobile tram system for systematic sampling of ecosystem optical properties. *Remote Sensing of Environment* 103:246–254.
- Gotelli, N. J., and R. K. Colwell. 2001. Quantifying biodiversity: procedures and pitfalls in the measurement and comparison of species richness. *Ecology Letters* 4:379–391.
- Gould, W. 2000. Remote sensing of vegetation, plant species richness, and regional biodiversity hotspots. *Ecological Applications* 10:1861–1870.
- Haddad, N. M., et al. 2009. Plant species loss decreases arthropod diversity and shifts trophic structure. *Ecology Letters* 12:1029–1039.
- Helmus, M. R., et al. 2007. Phylogenetic measures of biodiversity. *American Naturalist* 169:E68–E83.
- Heywood, V. H. 1995. *Global biodiversity assessment*. Cambridge University Press, Cambridge, UK.
- Jetz, W., et al. 2016. Monitoring plant functional diversity from space. *Nature Plants* 2:16024.
- John, R., et al. 2008. Predicting plant diversity based on remote sensing products in the semi-arid region of Inner Mongolia. *Remote Sensing of Environment* 112:2018–2032.
- Kembel, S. W., et al. 2010. Picante: R tools for integrating phylogenies and ecology. *Bioinformatics* 26:1463–1464.
- Kerr, J. T., et al. 2001. Remotely sensed habitat diversity predicts butterfly species richness and community similarity in Canada. *Proceedings of the National Academy of Sciences USA* 98:11365–11370.
- Legendre, P., and L. Legendre. 1998. *Numerical ecology*. Elsevier, Amsterdam, The Netherlands.
- Lord, D., et al. 1985. Influence of wind on crop canopy reflectance measurements. *Remote Sensing of Environment* 18:113–123.
- Lucas, K., and G. Carter. 2008. The use of hyperspectral remote sensing to assess vascular plant species richness on Horn Island, Mississippi. *Remote Sensing of Environment* 112:3908–3915.
- Magurran, A. E. 2004. *Measuring biological diversity*. Blackwell Publishing, Hoboken, New Jersey, USA.
- Magurran, A. E., and M. Dornelas. 2010. Biological diversity in a changing world. *Philosophical Transactions of the Royal Society B* 365:3593–3597.
- Marceau, D. J., and G. J. Hay. 1999. Contributions of remote sensing to the scale issue. *Canadian Journal of Remote Sensing* 25:357–366.
- Naeem, S., et al. 2000. Plant diversity increases resistance to invasion in the absence of covarying extrinsic factors. *Oikos* 91:97–108.
- Nagendra, H. 2001. Using remote sensing to assess biodiversity. *International Journal of Remote Sensing* 22:2377–2400.
- Nagendra, H. 2002. Opposite trends in response for the Shannon and Simpson indices of landscape diversity. *Applied Geography* 22:175–186.
- Oldeland, J., et al. 2010. Does using species abundance data improve estimates of species diversity from remotely sensed spectral heterogeneity? *Ecological Indicators* 10:390–396.
- Ollinger, S. V. 2011. Sources of variability in canopy reflectance and the convergent properties of plants. *New Phytologist* 189:375–394.
- O'Neill, R. V., and A. W. King. 1998. Homage to ST. Michael; Or, Why are there so many books on scale? Pages 3–15 *in* D. L. Peterson and V. T. Parker, editors. *Ecological scale: Theory and applications*. Columbia University Press, New York, New York, USA.
- O'Neill, R. V., et al. 1986. *A hierarchical concept of ecosystems*. Princeton University Press, Princeton, New Jersey, USA.
- Peet, R. K. 1974. The measurement of species diversity. *Annual Review of Ecology and Systematics* 5:285–307.
- Pereira, H. M., et al. 2013. Essential biodiversity variables. *Science* 339:277–278.
- Petchev, O. L., and K. J. Gaston. 2002. Functional diversity (FD), species richness and community composition. *Ecology Letters* 5:402–411.
- Pielou, E. C. 1966. The measurement of diversity in different types of biological collections. *Journal of Theoretical Biology* 13:131–144.
- Rocchini, D. 2007. Effects of spatial and spectral resolution in estimating ecosystem α -diversity by satellite imagery. *Remote Sensing of Environment* 111:423–434.
- Sanchez-Azofeifa, G. A., et al. 2009. Differences in leaf traits, leaf internal structure, and spectral reflectance between two communities of lianas and trees: Implications for remote sensing in tropical environments. *Remote Sensing of Environment* 113:2076–2088.
- Schäfer, E., et al. 2016. Mapping tree species diversity of a tropical montane forest by unsupervised clustering of airborne imaging spectroscopy data. *Ecological Indicators* 64:49–58.
- Shannon, C. E. 1948. A mathematical theory of communication. *Bell System Technical Journal* 27(379–423):623–656.
- Siemann, E., et al. 1998. Experimental tests of the dependence of arthropod diversity on plant diversity. *American Naturalist* 152:738–750.
- Simpson, E. H. 1949. Measurement of diversity. *Nature* 163:688.
- Srivastava, D. S., et al. 2012. Phylogenetic diversity and the functioning of ecosystems. *Ecology Letters* 15:637–648.
- Tilman, D. 1997. The influence of functional diversity and composition on ecosystem processes. *Science* 277:1300–1302. <http://doi.org/10.1126/science.277.5330.1300>
- Turner, W. 2014. Sensing biodiversity. *Science* 346:301–303.
- Turner, M. G., et al. 1989. Predicting across scales: Theory development and testing. *Landscape Ecology* 3:245–252.

- Turner, W., et al. 2015. Free and open-access satellite data are key to biodiversity conservation. *Biological Conservation* 182:173–176.
- Ustin, S. L. 2013. Remote sensing of canopy chemistry. *Proceedings of the National Academy of Sciences USA* 110:804–805.
- Ustin, S. L., and J. A. Gamon. 2010. Remote sensing of plant functional types. *New Phytologist* 186:795–816.
- Violle, C., et al. 2012. The return of the variance: Intraspecific variability in community ecology. *Trends in Ecology & Evolution* 27:244–252.
- Wang, R., et al. 2016a. Integrated analysis of productivity and biodiversity in a southern Alberta prairie. *Remote Sensing* 8:214.
- Wang, R., et al. 2016b. Seasonal variation in the NDVI–species richness relationship in a prairie grassland experiment (Cedar Creek). *Remote Sensing* 8:128.
- Whittaker, R. H. 1960. Vegetation of the Siskiyou Mountains, Oregon and California. *Ecological Monographs* 30: 279–338.
- Whittaker, R. H. 1972. Evolution and measurement of species diversity. *Taxon* 21:213–251.
- Williams, C. B. 1964. *Patterns in the balance of nature and related problems in quantitative ecology*. Academic Press, Cambridge, Massachusetts, USA.
- Woodcock, C. E., and A. H. Strahler. 1987. The factor of scale in remote sensing. *Remote Sensing of Environment* 21:311–332.
- Wright, I. J., et al. 2004. The worldwide leaf economics spectrum. *Nature* 428:821–827. <http://doi.org/10.1038/nature02403>
- Wu, J., and O. L. Loucks. 1995. From balance of nature to hierarchical patch dynamics: A paradigm shift in ecology. *Quarterly Review of Biology* 70:439–466.
- Zanne, A. E., et al. 2014. Three keys to the radiation of angiosperms into freezing environments. *Nature* 506:89–92.
- Zhang, Y., et al. 2012. Forest productivity increases with evenness, species richness and trait variation: A global meta-analysis. *Journal of Ecology* 100:742–749.

SUPPORTING INFORMATION

Additional supporting information may be found online at: <http://onlinelibrary.wiley.com/doi/10.1002/eap.1669/full>

DATA AVAILABILITY

Data available from EcoSIS and NASA LP DAAC: Whole plot spectral data (EcoSIS): <https://doi.org/10.21232/c2t66f>
Headwall images (LP DAAC): <https://doi.org/10.5067/community/headwall/hwhypccmn1mm.001>
Airborne images (LP DAAC): <https://doi.org/10.5067/community/airborne/aehypccmn300mm.001>